Numerical Simulation of Critical Factors Controlling Heat Extraction from Geothermal Systems Using a Closed-Loop Heat Exchange Method

Curtis M. Oldenburg[1], Lehua Pan[1], Mark P. Muir[2], Alan D. Eastman[2], Brian S. Higgins[2]

[1]Energy Geosciences Division 74-316C, Lawrence Berkeley National Laboratory, Berkeley, CA 94720

[2]Greenfire Energy, 4300 Horton Ave, Unit 15, Emeryville, CA 94608

cmoldenburg@lbl.gov, lpan@lbl.gov,

mark.muir@greenfireenergy.com, alan.eastman@greenfireenergy.com, brian.higgins@greenfireenergy.com

Keywords: Enter your keywords here. CO_2, numerical modeling, T2Well, TOUGH2, closed-loop, thermosiphon

ABSTRACT

Closed-loop heat exchange for geothermal energy production involves injecting working fluid down a well that extends through the geothermal resource over a significant length to absorb heat by conduction through the well pipe. The well then needs to return to the surface for energy recovery and fluid re-injection to complete the cycle. We have carried out mixed convective-conductive fluid-flow modeling using a wellbore flow model for TOUGH2 called T2Well to investigate the critical factors that control closed-loop geothermal energy recovery. T2Well solves a mixed explicit-implicit set of momentum equations for flow in the pipe with full coupling to the implicit three-dimensional integral finite difference equations for Darcy flow in the porous medium. T2Well has the option of modeling conductive heat flow from the porous medium to the pipe by means of a semi-analytical solution, which makes the computation very efficient because the porous medium does not have to be discretized. When the fully three-dimensional option is chosen, the porous medium is discretized and heat flow to the pipe is by conduction and convection, depending on reservoir permeability and other factors. Simulations of the closed-loop system for a variety of parameter values have been carried out to elucidate the heat recovery process. To the extent that convection may occur to aid in heat delivery to the pipe, the permeability of the geothermal reservoir, whether natural or stimulated, is an important property in heat extraction. The injection temperature and flow rate of the working fluid strongly control the ultimate energy recovery. Pipe diameter also plays a strong role in heat extraction, but is correlated with flow rate. Similarly, the choice of working fluid plays an important role, with water showing better heat extraction than CO_2 for certain flow rates, while the CO_2 has higher pressure at the production wellhead which can aid in surface energy recovery. In general, we find complex interactions between the critical factors that will require advanced computational approaches to fully optimize.

1. INTRODUCTION

There are many reasons that producing fluid directly from liquid-dominated geothermal systems is problematic, whether this is native fluid or a working fluid that is injected and produced for heat recovery (aka an open loop), for example: (1) the produced fluid may contain dissolved chemical components from the rock making it corrosive to the well and surface collection pipes; (2) produced fluid may transport chemical species (e.g., acid gases) from the reservoir to the surface where they must be handled as hazardous pollutants; (3) the produced fluid itself may be hazardous and require special handling or incur disposal costs; (4) injected working fluid may react with the rock and lead to formation damage, either excessively dissolving the reservoir or plugging it up; or (5) there may not be sufficient permeability in the geothermal reservoir to inject or recover working fluid at sufficient rates. One way to avoid these problems is to keep reservoir fluids isolated from the geothermal energy recovery infrastructure through the use of a closed-loop circulation system in which the working fluid never contacts the host rock.

Various configurations of systems exist to isolate the host rock and native geothermal fluids from working fluids for energy recovery. In the first class of designs, the circulation system is installed in a single vertical borehole. For example, one such downhole heat exchanger design has U-shaped tubing emplaced in boreholes with perforated casings (e.g., Lund, 2003). Another kind of device in a single borehole is the wellbore heat exchanger that includes open-hole sections for limited rock-fluid interaction in low-permeability host rock (e.g., Nalla et al., 2005). Another single wellbore configuration is the coaxial or tube-in-tube design (e.g., Horne, 1980; Wang et al., 2009) with insulated central tubing. Prior study of single-well closed-loop heat exchange systems using water as working fluid have concluded that the limitations of thermal conduction through the pipe and into the working fluid, combined with local thermal depletion of the reservoir around the pipe, limit the heat extraction capability of these systems (e.g., Nalla et al., 2005). However, recent developments in reservoir stimulation, drilling technology, and the use of novel working fluids, coupled with the imperative to lower environmental impacts of geothermal energy, are inspiring renewed interest in closed-loop systems.

In this study, we consider a wide U-shaped configuration with a significant horizontal portion to increase contact with the high-temperature reservoir as shown in Figure 1. The idea is that the reservoir in the horizontal section could be stimulated (e.g., by hydraulic fracturing) during well construction to enhance reservoir natural convection. Furthermore, many of these systems could be built in parallel to extract heat from the reservoir. In addition, while water is an excellent working fluid to extract heat, other fluids such as supercritical CO_2 may have significant advantages due to their expansion upon heating, which under certain conditions creates a thermosiphon that can entirely or partially eliminate the need for pumping and provides a high-pressure outlet stream that can be used to generate power. The purpose of this paper is to demonstrate the modeling capabilities that we have applied to such a system, and to

describe our modeling results that examine critical factors and their role in controlling performance of the U-shaped closed-loop heat exchanger using CO_2 as the working fluid.

We note that CO_2 at a given post-turbine pressure and temperature is assumed to be available at the wellhead for injection. In Figure 1, this CO_2 is shown available at 7.5 MPa and 75 °C. If a high flow rate in the well is desired, the CO_2 may have to be compressed just before injection into the well. This compression process will increase the injection temperature and pressure as will be shown in the results below. We note further that the U-shaped closed loop would require the use of horizontal drilling and careful ranging to create the long horizontal run of the well with vertical return sections, topics not discussed in this paper. In addition, while we assume a stimulated zone in some of our simulations, we address neither the process nor the cost of stimulating the reservoir in this study. Our study is focused on modeling and simulation of the flow and heat transfer processes involved in the U-shaped closed loop heat recovery system and does not address either surface energy recovery or economic feasibility.
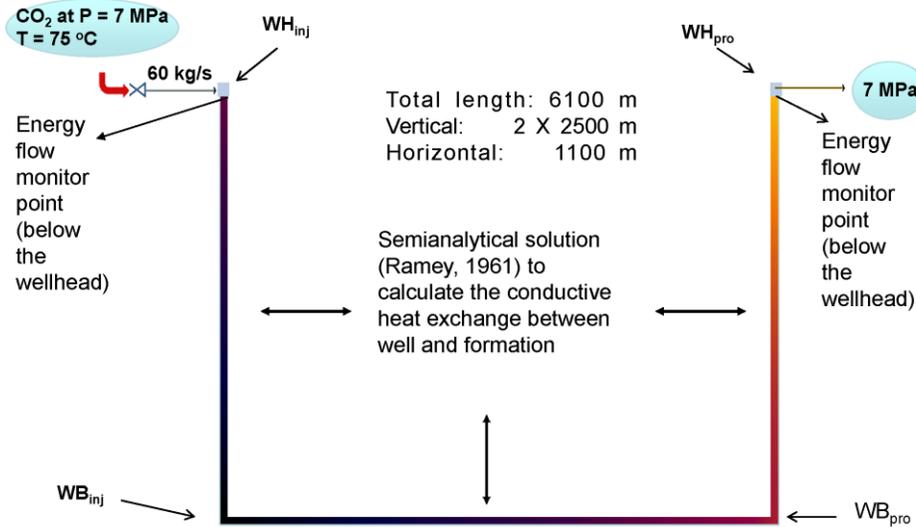

Figure 1: Sketch of closed loop geothermal energy system for CO_2 flowing from inlet (upper left-hand side) to outlet (upper right-hand side). WH_{inj} = wellhead of injection leg; WB_{inj} = wellbottom of injection leg; WB_{pro} = wellbottom of production leg; WH_{pro} = wellhead of production leg.

2. METHODS

Simulations of the closed-loop system are carried out using a member of the TOUGH (Pruess et al., 2001; 2012) family of codes called T2Well (Pan et al., 2011; Pan and Oldenburg, 2014). T2Well models flow in the wellbore by solving the 1D transient momentum equation of the fluid mixture with the drift-flux model (DFM), and flow in the reservoir using standard (multiphase) Darcy's law. Although we model compression and decompression in the well that takes CO_2 from supercritical to gaseous conditions, this is not formally a phase change. Therefore, we have only single-phase flow in the CO_2-filled pipe and in the liquid-dominated geothermal system. Because the CO_2 is isolated from the reservoir by the well casing, there is no advective coupling between the pipe and the reservoir. This is a greatly simplified system compared to the two-phase (CO_2-rich and H_2O-rich) wellbore-reservoir coupling processes which T2Well is capable of modeling (e.g., Oldenburg et al., 2012; Oldenburg and Pan, 2013). For single-phase conditions in the pipe, the transient momentum equation of CO_2 pipe flow, including temporal momentum change rate, spatial momentum gradient, friction loss to the pipe wall, gravity, and pressure gradient, is solved to obtain the velocity of flowing CO_2. In the reservoir, natural convection may occur depending on the permeability which limits convection and the buoyancy which drives it. In the case where the permeability of the reservoir is very small, heat transfer to the pipe is by conduction only, and the semi-analytical model of Ramey (1962) is used to model heat transfer between the reservoir and the fluid in the pipe. We refer to cases with only conduction in the reservoir as the "pipe-only" model. We use ECO2N V 2.0 (Pan et al., 2014) to model the thermophysical properties of CO_2 and water. Grid generation is carried out using WinGridder (Pan, 2003).

3. MODEL SYSTEM

3.1 Well

The U-shaped well consists of a long (1 km) horizontal leg within the reservoir connected to two 2.5 km-long vertical injection and production sections. Base-case properties of the well and CO_2-injection and production conditions are shown in Table 1. The total length of the well is 6 km. The working fluid (CO_2) is introduced at the inlet side (left-hand side in Figure 1) and produced out of the outlet on the right-hand side. Thermal conductivity of steel is 50.2 W/(m K), much higher than that of the reservoir rock and can therefore be ignored in the model.

Table 2. Properties of the (6-inch diameter) well.

	Value	Units	Parameter
Horizontal well (lateral)	1100	m	Length
	0.168 (6.61 inch)	m	Diameter
	0.154 (6.06 inch)	m	Tube I.D.
	steel	-	Material
	4.57×10^{-5}	m	Roughness factor
Vertical sections of well:	2500	m	Length
	0.168 (6.61 inch)	m	Diameter
	0.154 (6.06 inch)	m	Tube I.D.
	steel	-	Material
	4.57×10^{-5}	m	Roughness factor

3.2 Reservoir

The reservoir is assumed to be a liquid-dominated geothermal reservoir in permeable sediments at a depth of approximately 2500 m with hydrostatic pressure of 25 MPa and initial temperature of 250 °C. The discretized domain and the vertical sections of the well (red lines) are shown in Figure 2a. As shown, we model one-half of the system (mirror plane symmetry) along the axial direction of the horizontal section of the well and assume no heat or fluid flow occurs out of the lateral boundary, such as might be appropriate if there were a series of these U-shaped wells installed parallel to each other 100 m apart in the reservoir. Figure 2b shows a vertical cross section through the horizontal section of the well showing the graded discretization with refinement around the well. Note the 40 m x 40 m region around the well that will be modeled as a stimulated region in one of our scenarios. The details of the refinement around the well are shown in Figure 2c. We refined the grid to this extent to ensure that we would capture sharp temperature gradients between the reservoir and pipe that occur in cases of strong natural convection in the reservoir. In the case of the zero-permeability reservoir, we do not discretize the reservoir at all, but instead assume that heat transfer is by conduction as calculated using Ramey's (1962) semi-analytical solution. We always use the semi-analytical solution for heat transfer all along the vertical injection and production parts of the well to avoid having to discretize the overburden. Properties of the reservoir are presented in Table 2. We point out the set of simulations presented here assume a reservoir thermal conductivity of 4 W/(m °C), consistent with measurements of sandstone (e.g., Zimmerman, 1989).
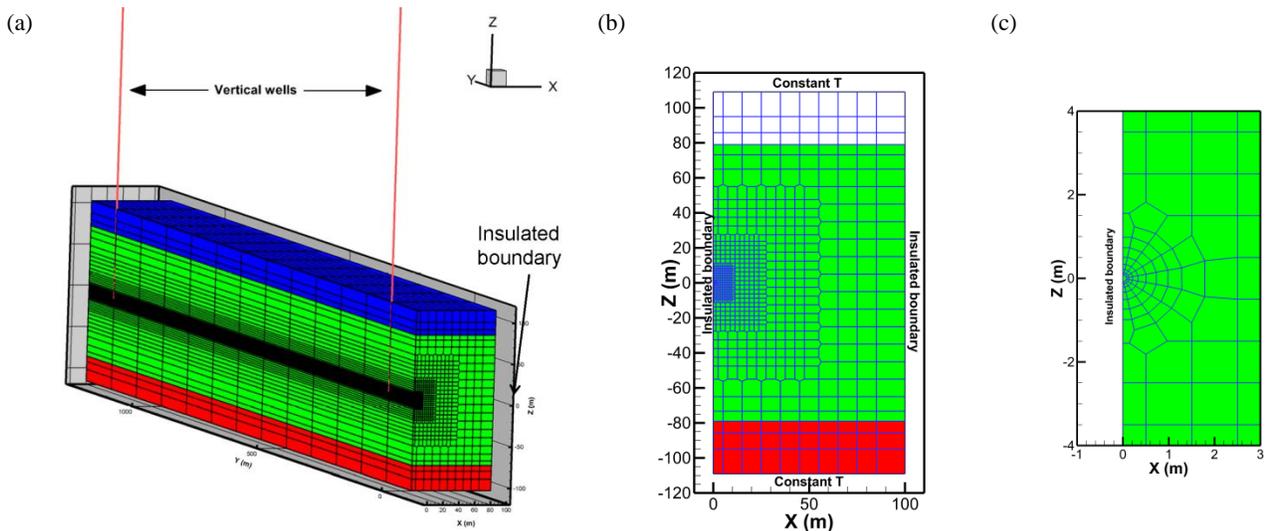

Figure 2: Discretization of the reservoir part of the closed-loop model showing (a) 3D domain (blue = overburden, red = underburden, and green = reservoir region) including the vertical legs (red lines) of the closed-loop well, (b) cross section of the horizontal well region, and (c) closeup of the well region.

Table 1. Properties of various regions of the closed-loop reservoir model.

Zone	Thickness (m)	Porosity (vol %)	Rock grain density (kg m^{-3})	Rock grain specific heat (J/(kg °C))	Thermal cond.* (W/(m °C))	Pore compress. (Pa^{-1})	k (Case 1) (m^2)	k (Case 2) (m^2)	k (Case 3) (m^2)
Overburden	155	5	2700	1000	4.0	7.25 x 10^{-12}	10^{-20}	10^{-15}	10^{-15}
Reservoir	158	25.4	2700	1000	4.0	7.25 x 10^{-12}	10^{-18}	10^{-12}	10^{-12}
Underburden	55	5	2700	1000	4.0	7.25 x 10^{-12}	10^{-20}	10^{-15}	10^{-15}
High-k zone around well	40	25.4	2700	1000	4.0	7.25 x 10^{-12}	10^{-18}	10^{-12}	10^{-10}

*under liquid-saturated conditions.

4. RESULTS

4.1 Full-reservoir (3D) base case

When CO_2 is injected at a specified rate into the well, it may either heat up as it compresses or cool down as it expands as controlled by its initial conditions, the injection rate, and the pipe flow capacity. This change in CO_2 pressure and temperature arises from how CO_2 is injected into the wellhead. In our conceptualization, CO_2 will be delivered to the wellhead from the energy recovery infrastructure at the surface, e.g., from the outlet of a turbine, at a certain pressure and temperature. These conditions may not be compatible with the desired flow rate for CO_2 through the U-shaped well. For CO_2 at 7 MPa and 75 °C injected at 60 kg/s into the 6-inch well, the CO_2 heats up to approximately 110 °C and attains a pressure of 12.5 MPa. In the thermosiphon scenario, no compression is used and the CO_2 from the outlet of the turbine flows freely down the well. Regardless of whether extra compression is needed or not, as CO_2 flows down the well into hot regions of the subsurface, its energy changes as it loses gravitational potential, heats up by compression and by absorbing heat through the hot pipe wall, and as its velocity changes. These four forms of energy, pressure-volume, thermal, kinetic, and gravitational potential are all accounted for in T2Well in the output energy gain (MW) that we will report below. We note that because mass is conserved in the pipe, and the inlet is at the same elevation as the outlet, the gravitational potential energy difference across the system is always zero.

Results of energy gain for CO_2 flowing through the pipe-reservoir system for Cases 1, 2, and 3 for the full-reservoir (3D) system are shown in Figure 3. The low-k and standard-k (Cases 1 and 2, respectively) cases both produce about 1.75 MW at nearly steady state. In the low-k case (Case 1), convection is negligible in the reservoir. The small differences between Cases 1 and 2 show that convective heat transfer is not very important for the reservoir with 1 Darcy permeability. On the other hand, Case 3, with a high-k zone around the well, produces about twice as much energy as Cases 1 and 2 and demonstrates that natural convection in the reservoir can greatly enhance energy recovery. We note also in Figure 3a that the thermal resource is not appreciably depleted over the 30 years of simulation for the non-stimulated case. The model system has a constant-temperature boundary condition at the bottom that serves to replenish heat. For Case 3 with stimulated near-well region, Figure 3b shows that the energy gain declines over time as local convective heat transfer to the pipe appears to exceed the conductive heat transfer into the near-well region needed to replenish extracted heat.

Temperature along the well is shown for the three cases in Figure 3b. The temperature profile "Geo T" represents the ambient (no-flow, or initial) pipe temperature, which reflects the geothermal gradient in the vertical parts of the well and the reservoir temperature in the horizontal parts of the well. When CO_2 is injected the temperature in the well is lower than the initial temperature everywhere except near the tops of the inlet and outlet sides of the well. This shows that there is potential for heating of the CO_2 all along the well except at shallow depths near the inlet and outlet points. The data for Case 3 in this figure demonstrate the strong benefit of the convective heat transfer that occurs if the near-well region can be stimulated to support natural convection.
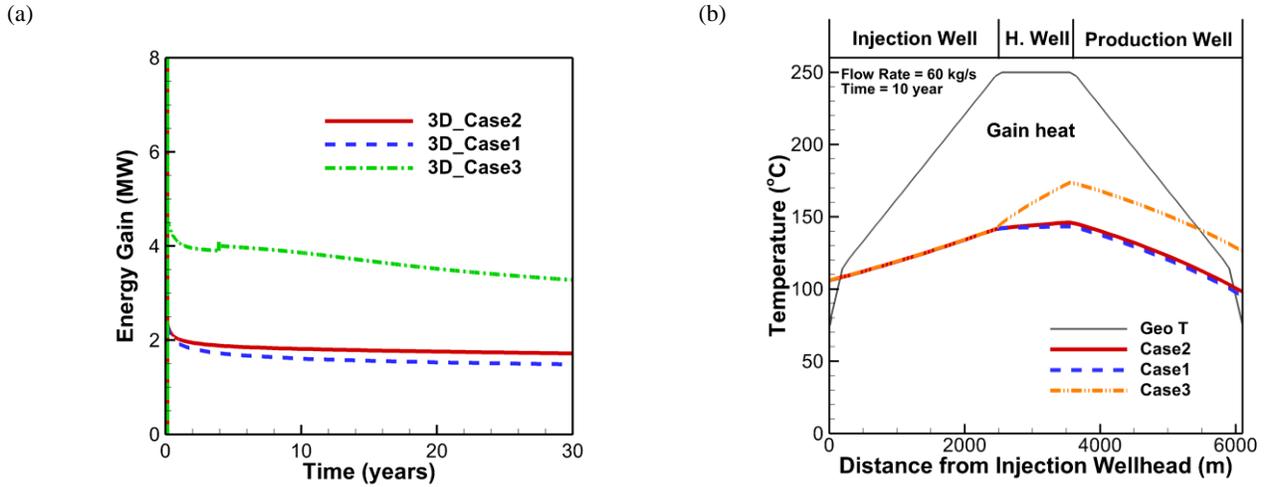
(a)

(b)

Figure 3: Simulation results of the effect of reservoir permeability on energy gain in the closed loop. (a) High-permeability in the reservoir favors convective heat transfer to the pipe. (b) The effects of convective heat transfer to the pipe are largest in the horizontal section of the closed loop.

The effect of different initial CO_2 temperatures is shown in Figure 4. If the CO_2 is initially at 40 °C instead of 75 °C prior to compression and injection into the well, it ends up leaving the well having gained more energy due to the larger temperature difference between the working fluid and reservoir. Figure 4 shows approximately 50% improvement in energy gain for the lower temperature CO_2 (Figure 4a). However, the production temperatures of the 40 °C case are still significantly cooler (Figure 4b) than for the 75 °C case. We conclude that starting with colder CO_2 is advantageous for increasing the energy gained by the flowing CO_2.
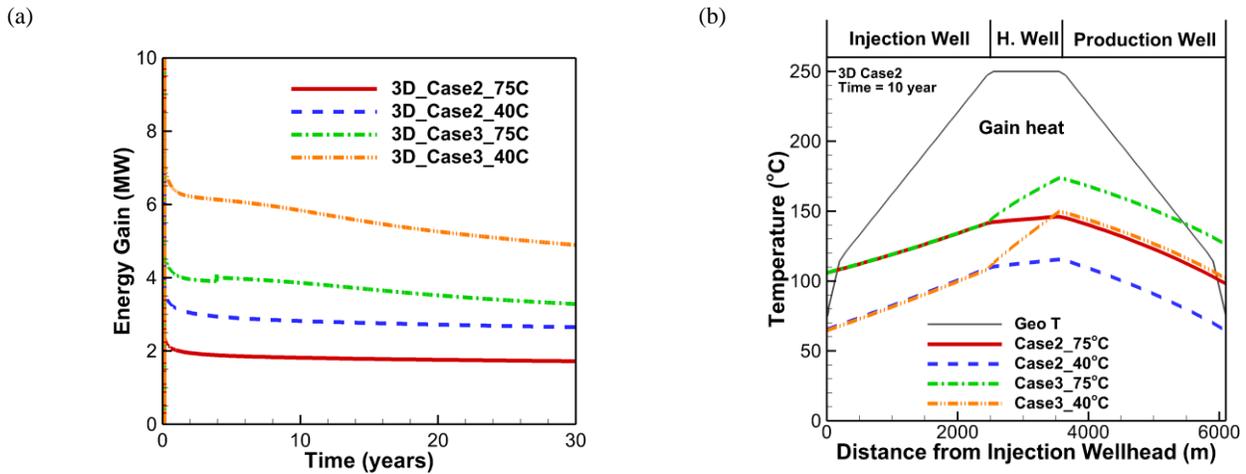
(a)

(b)

Figure 4: Simulation results of the effect of different inlet CO_2 temperatures on energy gain in the closed loop for the low-permeability (Case 2) and high-permeability (Case 3) reservoirs. (a) Low inlet temperature improves energy recovery; (b) Heating due to convection of heat from reservoir to CO_2 occurs for high-permeability (Case 3) reservoir.

The next variation we show is flow rate. As seen in Figures 5a and 5b, energy recovery may be lower for either higher or lower injection flow rates. For CO_2 as the working fluid, the reasons are more complicated than for a nearly incompressible fluid such as water, for which a similar effect was observed but for different reasons by Nalla et al. (2004). Specifically, for water with all other things equal, the flow rate can be so small that the fluid heats up too much thereby reducing the temperature difference between fluid and reservoir at the downstream ends of the well, resulting in little energy recovery. Or the flow rate may be so high that not enough time is allowed for water to efficiently absorb heat during its rapid flow through the pipe. In short, flow rate alone leads to an optimal flow rate in a water-based system. For CO_2 on the other hand, the situation is more complicated because CO_2 density can change significantly as it heats up and expands during flow in the pipe, leading to changes in velocity even though mass flow rate is constant. Nevertheless, there is an optimum flow rate for CO_2 to maximize energy gain. The initial temperature of the injected CO_2 plays the same general role as it does for water in that colder initial temperatures lead generally to better heat gain. But for CO_2, both the effects of flow rate and initial temperature affect energy gain. As shown in Figure 5a, the 60 kg/s case is better than either the 30 kg/s or 90 kg/s cases, even though the 60 kg/s case is not the coldest (Figure 5b).
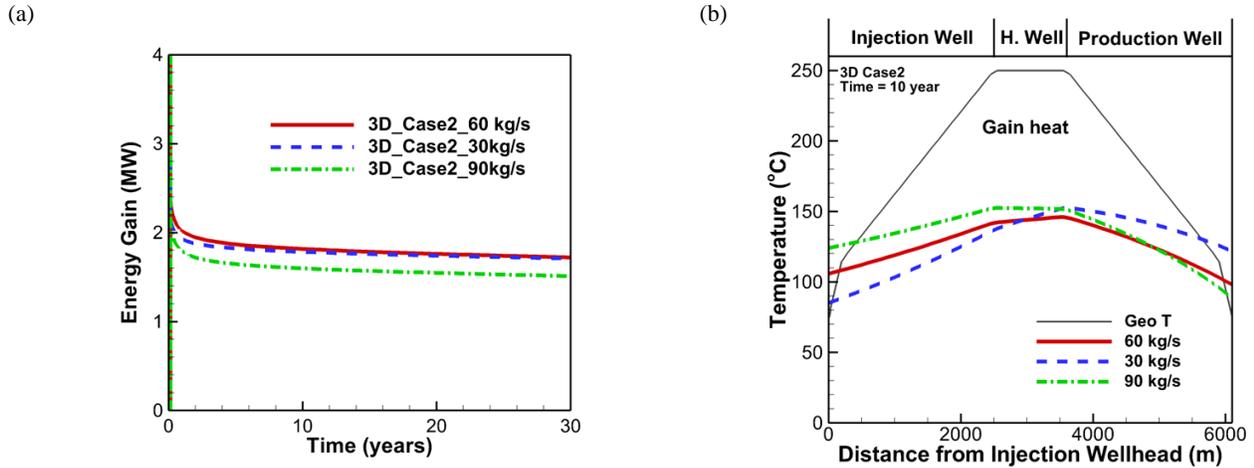
(a)

(b)

Figure 5: Simulation results of the effect of different CO_2 flow rates on energy gain in the closed loop for the low-permeability (Case 2) reservoir. (a) Intermediate flow rate (60 kg/s) is better than 30 kg/s or 90 kg/s for energy recovery; (b) Only the low flow-rate case results in CO_2 temperature higher at outlet than at inlet of closed loop.

Another obvious factor in energy gain along the pipe is the pipe surface area. Another complication arises here with pipe diameter as a parameter because mass flow rate and pipe diameter are strongly correlated. As shown in Figure 6a, the best combination from among what we tested was 60 kg/s with a 10-inch pipe. Note that the 10-inch pipe is also the best choice if one fixes the injection rate at 48 kg/s (Figure 6a), and that the 10-inch pipe produces the highest outlet temperature at fixed injection rate (Figure 6b).
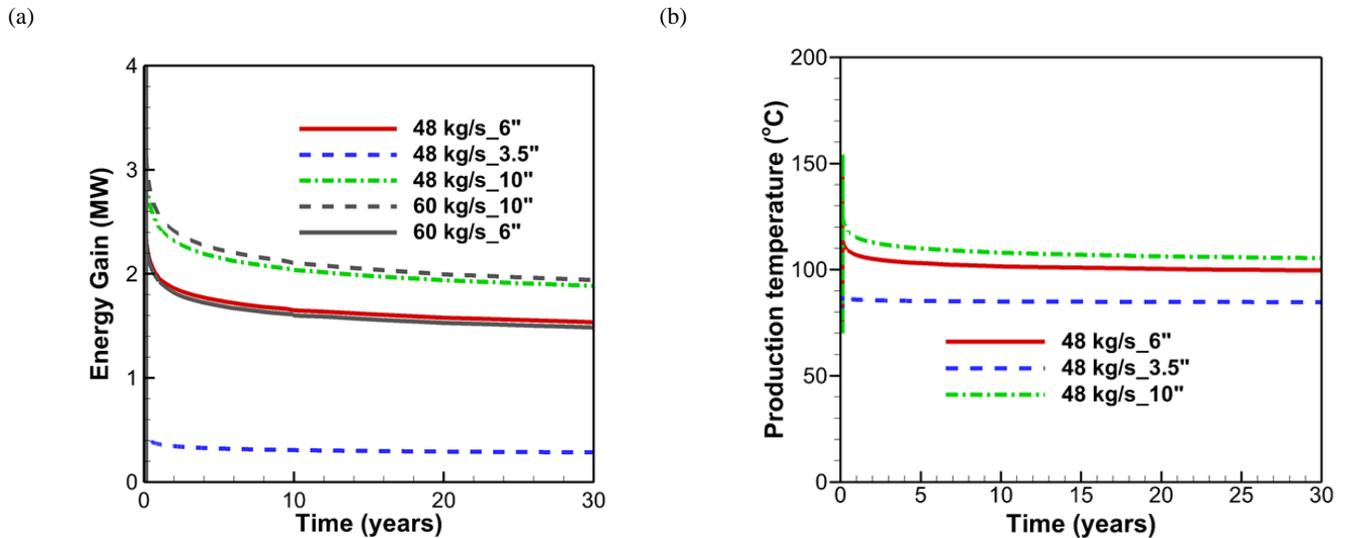
(a)

(b)

Figure 6: Simulation results of the effect of pipe diameter on energy gain in the closed loop. (a) High flow rates in large-diameter pipes favor heat transfer to the pipe. (b) At fixed flow rate, larger temperatures develop in larger-diameter pipes in the closed loop.

We mentioned the behavior of water above in a hypothetical context, but we compared water with CO_2 explicitly also. We show in Figure 7 a comparison of CO_2 and water at the same mass flow rate in the closed-loop system. We observe that water gains more energy through the system than CO_2 does because it starts out with a smaller temperature so there is greater heat conduction to the water in the pipe during its passage through the reservoir. Furthermore, we observe that the water temperature steadily rises as it flows through the pipe, arriving at the outlet of the production well as hot water. The greater energy gain might be seen at first as an advantage over CO_2, but the fact is that the water simply heats up in the system. On the other hand, the CO_2 goes from supercritical form to high-pressure gaseous form at the outlet which means it can potentially spin a turbine for efficient energy conversion; that is not possible for water under the same conditions.
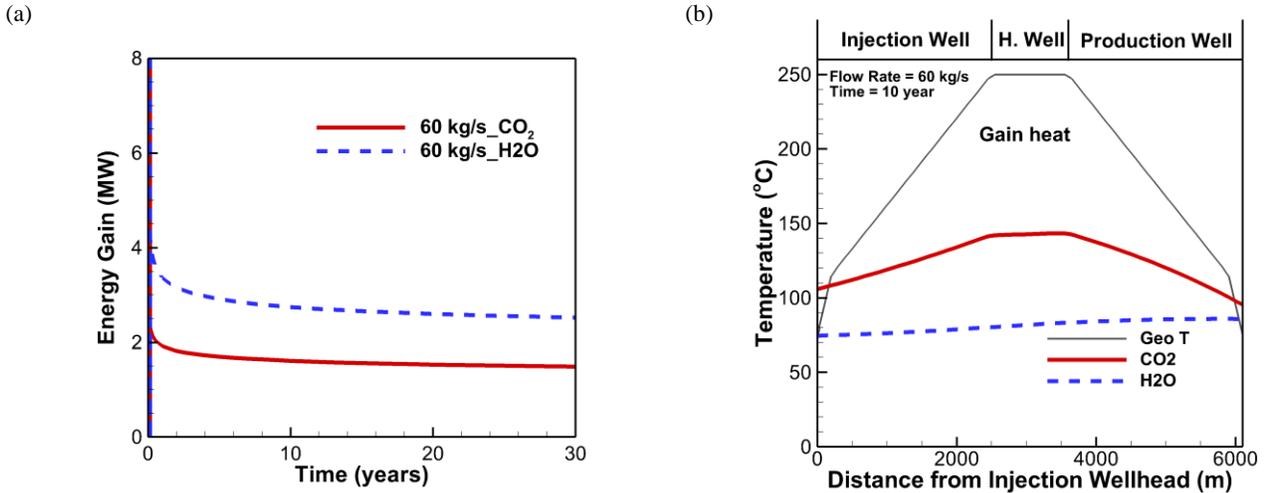
6

(a)

(b)

Figure 7: Simulation results for CO_2 and H_2O as working fluids. (a) Water gains more energy through the loop at 60 kg/s than CO_2. (b) Water temperature increases in each part of the closed loop whereas CO_2 temperature may decline due to decompression effects.

As might be inferred from the above comparison, the transition of CO_2 from supercritical to gaseous form during passage through the closed loop also enables a thermosiphon. In this variation, we investigate the flow rates that can be sustained solely by thermosiphon assuming CO_2 arrives at the injection well at a temperature of 35 °C. As shown in Figure 8a, energy gain will be in the range of 2.5 MW at steady state, with a thermosiphon possible for flow rates up to approximately 25 kg/s (Figure 8b). This analysis considered only the subsurface part of the closed loop; losses during energy recovery (e.g., the heat rejection equipment) will lead to a slightly smaller sustainable thermosiphon flow rate.
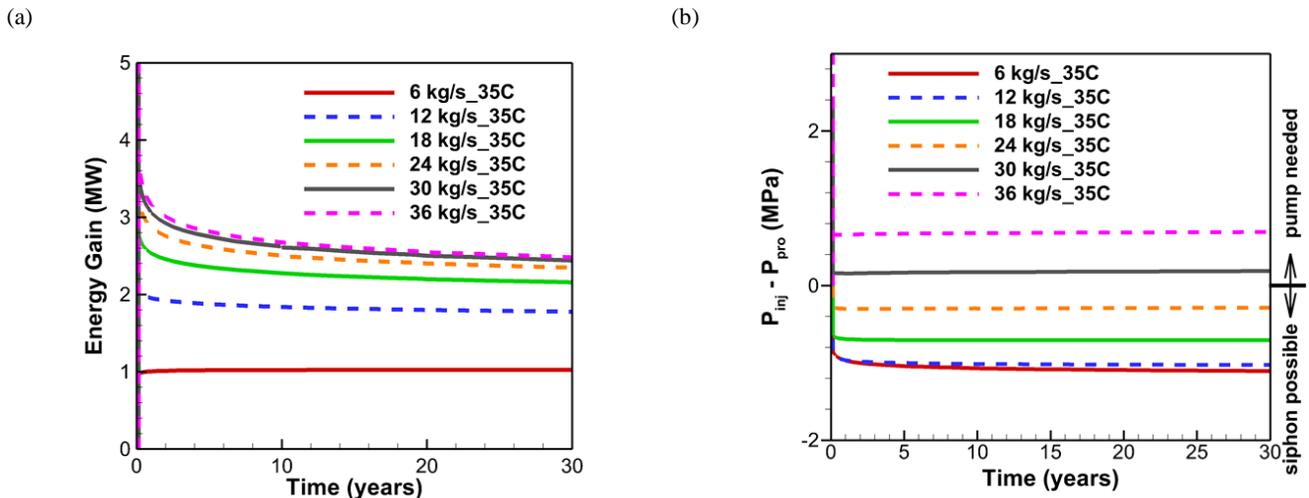
(a)

(b)

Figure 8: Simulation results for various CO_2 flow rates. (a) Energy gain correlates directly with flow rate at 35 °C inlet temperature. (b) The closed loop will operate without need for pump only at flow rates below about 25 kg/s.

5. CONCLUSIONS

We have used a detailed coupled pipe-reservoir model to investigate the effects of various parameters on the energy gain of CO_2 flowing in a U-shaped well through a geothermal reservoir. Reservoir permeability is a primary control on energy gain by the working fluid, with natural convection strongly favoring heat transfer to fluid in the pipe. Because of compressibility, the energy gain by flowing CO_2 in the pipe is a complicated function of initial temperature, flow rate, and pipe diameter. Considering the generation and sustainability of a thermosiphon, we find a flow rate of about 25 kg/s is the most that can be sustained in a 6-inch pipe with 35 °C CO_2 available at injection wellhead. Variables considered included pipe diameter, well depth, horizontal well length, temperature gradients, flow rates, and pressures. Based on the unique compressibility of supercritical CO_2 that can produce a thermosiphon, further modeling is warranted of CO_2 as a working fluid for closed-loop heat extraction, particularly using iTOUGH2 (Finsterle, 1999; 2005) optimization techniques to determine the best combination of parameters to maximize energy gain and above-ground power production.

Oldenburg, Pan, Muir, Eastman, Higgins

REFERENCES

Finsterle, S., 1999. iTOUGH2 user's guide. *LBNL-40040*, p.130.

Finsterle, S., Demonstration of optimization techniques for groundwater plume remediation using iTOUGH2, *Environmental Modelling and Software*, *21*(5), 665–680, doi:10.1016/j.envsoft.2004.11.012, 2005.

Horne, R.N., Design considerations of a downhole coaxial geothermal heat exchanger, *Geothermal Resources Council Transactions*, *4*, 569, 1980.

Lund, J.W., 2003. The use of downhole heat exchangers. Geothermics, 32(4), pp.535-543. Pan, L., and C.M. Oldenburg. "T2Well—An integrated wellbore–reservoir simulator." *Computers & Geosciences 65* (2014), 46-55.

Nalla, G., Shook, G.M., Mines, G.L. and Bloomfield, K.K., 2005. Parametric sensitivity study of operating and design variables in wellbore heat exchangers. *Geothermics*, *34*(3), pp.330-346.

Oldenburg, C.M., and L. Pan, Porous Media Compressed-Air Energy Storage (PM-CAES): Theory and Simulation of the Coupled Wellbore–Reservoir System, *Transport in Porous Media*, *97*(2) 201-221, 2013.

Oldenburg, C.M., B.M. Freifeld, K. Pruess, L. Pan, S. Finsterle, and G.J. Moridis. Numerical simulations of the Macondo well blowout reveal strong control of oil flow by reservoir permeability and exsolution of gas. *Proceedings of the National Academy of Sciences 109*, no. 50 (2012): 20254-20259.

Pan, L., 2003. Wingridder-an interactive grid generator for TOUGH2. Lawrence Berkeley National Laboratory.Pan, L., and C.M. Oldenburg. "T2Well—An integrated wellbore–reservoir simulator." *Computers & Geosciences 65* (2014), 46-55.

Pan, L., C.M. Oldenburg, Y. Wu, and K. Pruess, T2Well/ECO2N Version 1.0: Multiphase and Non-Isothermal Model for Coupled Wellbore-Reservoir Flow of Carbon Dioxide and Variable Salinity Water, Lawrence Berkeley National Laboratory Report *LBNL-4291E*, 2011.

Pan, L., Spycher, N., Doughty, C. and Pruess, K., 2014. ECO2N V. 2.0: A New TOUGH2 Fluid Property Module for Mixtures of Water, NaCl, and CO_2. Ernest Orlando Lawrence Berkeley National Laboratory Report *LBNL-6930E*, Berkeley, CA (US).

Pruess, K., C.M. Oldenburg, and G.J. Moridis. TOUGH2 User's Guide Version 2. E. O. Lawrence Berkeley National Laboratory Report *LBNL-43134*, 1999; and *LBNL-43134* (revised), 2012.

Pruess, K., 2010. Enhanced geothermal systems (EGS) with CO_2 as heat transmission fluid--A scheme for combining recovery of renewable energy with geologic storage of CO_2. Lawrence Berkeley National Laboratory.

Ramey Jr, H.J., 1962. Wellbore heat transmission. *Journal of Petroleum Technology*, *14*(04), pp.427-435.

Wang, Z., McClure, M.W. and Horne, R.N., 2009. A single-well EGS configuration using a thermosiphon. In *Workshop on Geothermal Reservoir Engineering*, Stanford University, Stanford, CA.

Zimmerman, R.W., 1989. Thermal conductivity of fluid-saturated rocks. *Journal of Petroleum Science and Engineering*, *3*(3), pp.219-227.